Journal of Power Sources 195 (2010) 2166–2173

Contents lists available at ScienceDirect

Journal of Power Sources

journal homepage: www.elsevier.com/locate/jpowsour

A novel crosslinking strategy for preparing poly(vinyl alcohol)-based proton-conducting membranes with high sulfonation

Chun-En Tsai [a], Chi-Wen Lin [b], Bing-Joe Hwang [a,c,*]

[a] Nanoelectrochemistry Laboratory, Department of Chemical Engineering, National Taiwan University of Science and Technology, Taipei 106, Taiwan
[b] Department of Chemical Engineering, National Yunlin University of Science and Technology, Yunlin, Taiwan
[c] National Synchrotron Radiation Research Center, Hsinchu 300, Taiwan

ARTICLE INFO

Article history:
Received 21 August 2009
Received in revised form 20 October 2009
Accepted 20 October 2009
Available online 30 October 2009

Keywords:
Poly(vinyl alcohol)
Proton-conducting membrane
Sulfonation
Two-step crosslinking process

ABSTRACT

This study synthesizes poly(vinyl alcohol) (PVA)-based polymer electrolyte membranes by a two-step crosslinking process involving esterization and acetal ring formation reactions. This work also uses sulfosuccinic acid (SSA) as the first crosslinking agent to form an inter-crosslinked structure and a promoting sulfonating agent. Glutaraldehyde (GA) as the second crosslinking agent, reacts with the spare OH group of PVA and forms, not only a dense structure at the outer membrane surface, but also a hydrophobic protective layer. Compared with membranes prepared by a traditional one-step crosslinking process, membranes prepared by the two-step crosslinking process exhibit excellent dissolution resistance in water. The membranes become water-insoluble even at a molar ratio of SO_3H/PVA–OH as high as 0.45. Moreover, the synthesized membranes also exhibit high proton conductivities and high methanol permeability resistance. The current study measures highest proton conductivity of 5.3×10^{-2} S cm^{-1} at room temperature from one of the synthesized membranes, higher than that of the Nafion® membrane. Methanol permeability of the synthesized membranes measures about 1×10^{-7} cm^2 S^{-1}, about one order of magnitude lower than that of the Nafion® membrane.

1. Introduction

Fuel cells have recently occupied an important position as next generation type clean energy sources. Hydrogen and direct methanol fuel cells (DMFC) are recognized among several kinds of fuel cells to utilize proton-conducting membranes. Until now, the perfluorinated ionomer, Nafion®, composed of poly(tetrafluoroethylene) backbones with perfluorinated pendant chains terminated by sulfonic acid has been widely used as an electrolyte in hydrogen as well as DMFC due to its exceptional chemical, thermal and mechanical stability and high proton conductivity. However, its high cost cell components and unstable properties at high temperature and high methanol permeability hinder complete application of this technology [1,2]. The barrier property to fuel methanol requires the solid polymer electrolyte membrane used in the DMFC, or reduced permeability (crossover) of fuel methanol from the anode side of the membrane to the cathode side [3]. For practical hydrogen fuel cell application, membrane hydration is critical for attaining higher proton conductivity because it enhances proton dissociation and formation of continuous clusters for proton transfer. The hydrated membranes of perfluorosulfonic acid polymers have high proton conductivity, and proton conductivity exhibits by channel structure generation caused by hydration (hydrated proton conduction). In other words, proton conduction takes place through water as a medium in hydrated membranes of perfluorosulfonic acid polymers, so that a specified amount of water exists in the hydrated membranes. Accordingly, methanol having high affinity with water easily passed through the membranes, so that the hydrated membranes of perfluorosulfonic acid polymers are limited with regard to the methanol barrier property [3]. The literature has discussed a high proton-conducting Nafion®/–SO_3H functionalized mesoporous silica composite membrane, indicating methanol permeability at 4.5×10^{-6} cm^2 S^{-1} [4]. Previous studies have used a sulfonation agent such as sulfoacetic acid or 4-sulfophthalic acid together with a crosslinking agent of sulfosuccinic acid (SSA) with sulfonic acid group and –COOH groups to prepare a PVA-based solid polymer electrolyte [5,6]. Many literatures discuss the organic–inorganic hybrid membranes containing sulfonic acid groups introduced by various sulfonation agents using a sol–gel process under acidic conditions [7–10]. Kim et al. [9] have synthesized PVA/sulfosuccinic acid (SSA)/silica hybrid membranes with different SSA contents. Methanol permeability ranged between 10^{-8} and 10^{-7} cm^2 S^{-1} and

* Corresponding author at: Nanoelectrochemistry Laboratory, Department of Chemical Engineering, National Taiwan University of Science and Technology, #43, Keelung Rd. Sec. 4, Taipei 106, Taiwan. Tel.: +886 2 27376624; fax: +886 2 27376644.
E-mail address: bjh@mail.ntust.edu.tw (B.-J. Hwang).

0378-7753/$ – see front matter © 2009 Elsevier B.V. All rights reserved.
doi:10.1016/j.jpowsour.2009.10.055

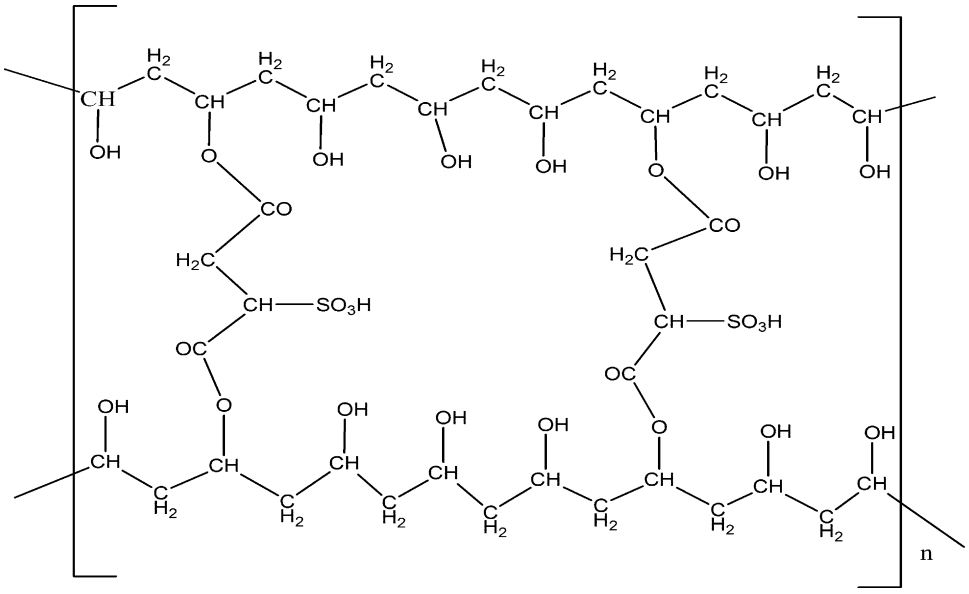

Scheme 1. Possible crosslinking structure of PVA and SSA.

proton conductivities ranged between 10^{-3} and 10^{-2} S cm^{-1} [9]. Crosslinked PVA/SSA/poly(acrylic acid)(PAA)/silica hybrid membranes have also been prepared using a chemical crosslinking agent having sulfonic acid group (–SO_3H), thereby increasing proton conductivity, and decreasing methanol permeability simultaneously. Previous studies report methanol permeability ranging between 10^{-8} and 10^{-7} cm^2 S^{-1} and proton conductivities ranging between 10^{-3} and 10^{-2} S cm^{-1} for organic/inorganic membranes [10]. Polymer family membranes have been prepared and evaluated as proton-conducting materials based on binary chemical crosslinking [11]. A two-polymer composite forms an interpenetrating polymer network (IPN) composed of proton-conducting 2-acrylamido-2-methyl-1-propanesulfonic acid (PAMPS) and a second polymer, poly(vinyl alcohol), serves as a methanol barrier. Adjusting polymer ratios and two-polymer crosslinking controls ion conductivity and methanol permeability uses dialdehydes [11,12] as the crosslinking agent. Kang et al. [13] and Kim et al. [14] prepared a proton exchange membrane using polymer blends of poly(vinyl alcohol) and poly(styrene sulfonic acid-co-maleic acid) (i.e. PVA/PSSA-MA). The semi-interpenetrating network (semi-IPN) based on crosslinking poly(vinyl alcohol) with sulfosuccinic acid (SSA) as a crosslinking agent and poly(styrene sulfonic acid-co-maleic acid) (PSSA-MA) as a proton source, forms a (semi-IPN) PVA/SSA/PSSA-MA membrane [15,16]. The PVA/SSA crosslinking structure is represented by the following general Scheme 1 [5,6].

The SSA as a crosslinking agent increases proton conductivity of PVA-based polymer electrolyte membranes and simultaneously reduces methanol permeability. Unfortunately, such an esterizing crosslinking bond is easily hydrolyzed by acid H^+. The single/bridge esterization ratio between PVA and SSA molecules increases with the amount of SSA [6]. A PVA/SSA membrane dissolves when the SSA crosslinking agent content is more than approximately 10 mole% based on PVA–OH. The organic–inorganic hybrid membranes of PVA/SSA/silica contain lower proton conductivity, therefore the suitable control of phase separation

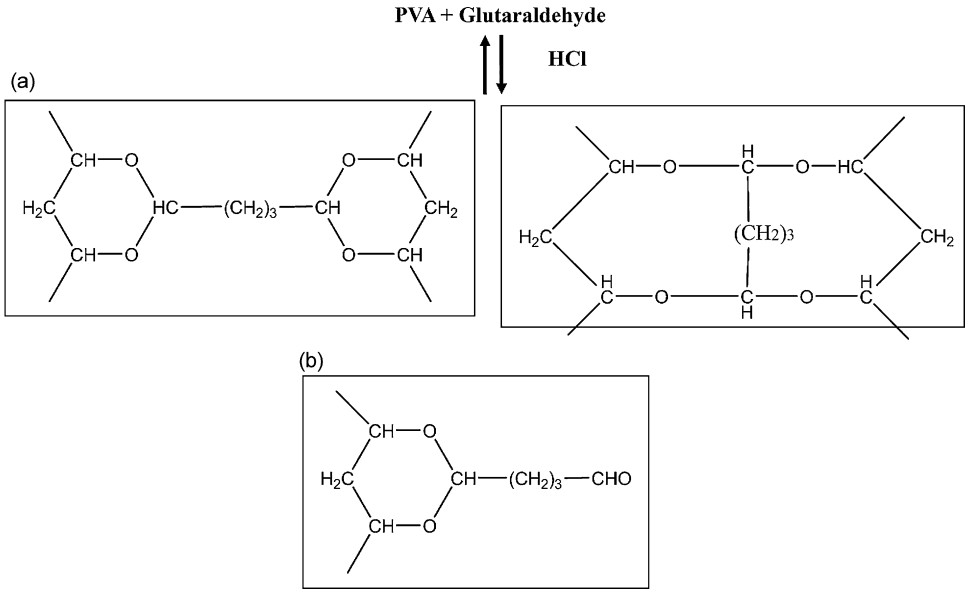

Scheme 2. Crosslinking PVA formed by reaction between PVA and GA: (a) acetal ring group or ether linkage and (b) aldehyde formation by monofunctional reaction.

is difficult. The above membrane becomes brittle and crackly when using a large amount of SSA crosslinking agent or silica [7–10]. The interpenetrating polymer network (IPN), composed of PVA/PAMPS crosslinked by dialdehyde, possesses high methanol permeability [11,12]. The above-mentioned electrolyte membrane associated with one crosslinking process has either low proton conductivity or a lower methanol barrier. This investigation seeks to increase SSA amount to form inner-hydrophilic crosslinking (called first crosslinking) based on PVA, thus increasing proton conductivity. Then, using glutaraldehyde (GA) as the second crosslinking agent to form outer-hydrophobic crosslinking of the membrane increases the methanol barrier. The following Scheme 2 represents glutaraldehyde crosslinking with PVA [17].

2. Experimental

2.1. Materials and membrane preparation

A solution-cast method forms the membranes. The stock PVA (99% hydrolyzed, average Mw = 124,000–186,000, Aldrich) and aqueous solution are prepared by dissolving 5 g of PVA into about 80 mL of DI water and then heating it to 70 °C with continuous stirring until obtaining a transparent solution.

2.1.1. First-chemical crosslinking of PVA–SSA

This work selects various molar ratios of SSA–SO_3H (sulfosuccinic acid, SSA)/PVA–OH, heated to about 70 °C with continuous stirring for at least 6 h, obtaining a cast solution. The cast solution is cast on plastic dishes, with water evaporated in an oven at 38 °C until visually dry. The membrane is then peeled from the plastic substrate, obtaining sulfonating and esterizing crosslinking thin membranes.

2.1.2. Second chemical crosslinking of PVA–SSA–GA

Samples of polymer membranes are separately soaked in 0.5 M glutaraldehyde/acetone reaction solution. Crosslinking occurs between the hydroxyl groups of PVA and the aldehyde groups of glutaraldehyde (GA), and catalyzed by sulfonic acid, deriving from sulfosuccinic acid (SSA). The acetal ring group or ether linkage forms following the second step of the crosslinking process. Acetone purifies the membranes before being placed in a vacuum oven for heat treatment. The second step of the crosslinking process for 1 h is denoted by C1 and 2 h is denoted by C2. Heat treatment for 1 h is denoted by H1 and 2 h is denoted by H2.

2.2. Infrared spectra measurements

Infrared spectra of the crosslinking PVA membranes are measured with an ATR IR spectroscope. A MIRacle™ Single Reflection HATR Spectrometer records attenuated total reflectance infrared (ATR IR) spectra of the membranes. The MIRacle™ is the PIKE Technologies Single Reflection Horizontal ATR (HATR) designed for use in FTIR spectrometers. The accessory sampling plate features a small round crystal allowing reliable sampling analysis, and the sampling plate comes in two configuration-polished ZnSe crystals. The membrane is squeezed between the ZnSe crystals and a pressing counterpart device with a micrometer-controlled compression clamp to achieve perfect contact.

2.3. Thermal analysis

Differential scanning calorimetry (DSC-6200, SII Nano Technology Inc.) and thermogravimetry (TG/DTA-6200, SII Nano Technology Inc.) perform thermal analysis of the polymer membranes. All measurements are performed under nitrogen. This study uses TGA data showing thermal degradation onset temperature of the samples as a reference for DSC measurements. The DSC measurements are carried out in a dry nitrogen atmosphere from 25 to 250 °C for membranes. The samples of about 5 mg are placed into aluminum pans, and heated to the desired temperature with a heating rate of 10 °C min^{-1} for TGA measurements and a heating rate of 5 °C min^{-1} for DSC measurements. The vacant aluminum pan serves as a reference during the whole experiment.

2.4. Swelling behavior of the measurements

Membrane swelling evaluation uses water uptake (WU) of the membranes (g g^{-1}), estimated from mass change before and after complete membrane dryness. The experiment swells the membranes in distilled water for more than two days, followed by carefully wiping the surface water with a filter paper (or wipe paper) and immediately weighing the membranes. The membranes are then dried in a vacuum oven at 80 °C for more than 48 h. The WU is thus calculated using the expression

$$\mathrm{WU} = \frac{W_{\mathrm{wet}} - W_{\mathrm{dry}}}{W_{\mathrm{dry}}}$$

where W_{wet} is the mass of the water-swollen membranes and W_{dry} is the mass of the dry membranes.

2.5. Ion exchange capacity

Titration determines ion exchange capacity (IEC; mequiv. g^{-1}) of the membranes as reported elsewhere [11,18]. Pieces of each membrane are soaked in 30 mL of a 2 M NaCl solution and equilibrated for at least 48 h to replace the protons by sodium ions. The remaining solution is then titrated with a 0.1 M NaOH solution using phenolphthalein as an indicator. The experiment defines the IEC as milliequivalents of sulfonic groups per gram of dried sample.

2.6. Water state

Melting transitions in DSC measurements detect two types of water in the membranes, freezing and nonfreezing (bound water), as described elsewhere [19,20]. Samples are first cooled from +25 to −40 °C with a cooling rate of 10 °C min^{-1}, and then heated at the rate of 2 °C min^{-1} up to +40 °C. Integrating the peak area of the melt endotherm obtains bulk water calculations in the samples. This work uses the degree of crystallinity in the water, obtained from the fusion heat of pure ice, 334 J g^{-1}, as a standard [11,19,20].

2.7. Proton conductivity measurement

Proton conductivity (σ) of polymer membranes is measured by an ac impedance technique using an electrochemical impedance analyzer (S-1260, Solartron), where the ac frequency is scanned from 100 kHz to 1 Hz at a voltage amplitude of 10 mV. Fully hydrated membranes are sandwiched into a conductivity equipped with a Pt foil electrode. Impedance is measured at a temperature maintained at 30 °C.

2.8. Methanol permeability measurements

This study determines methanol permeability of electrolyte measured using a homemade side-by-side diffusion cell. Before

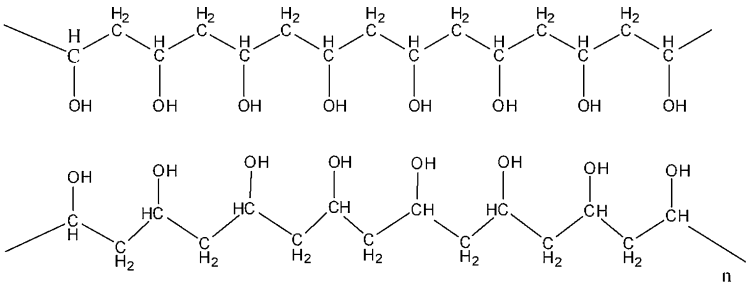

PVA

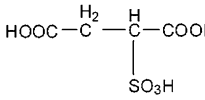

Sulfosuccnic Acid (SSA)

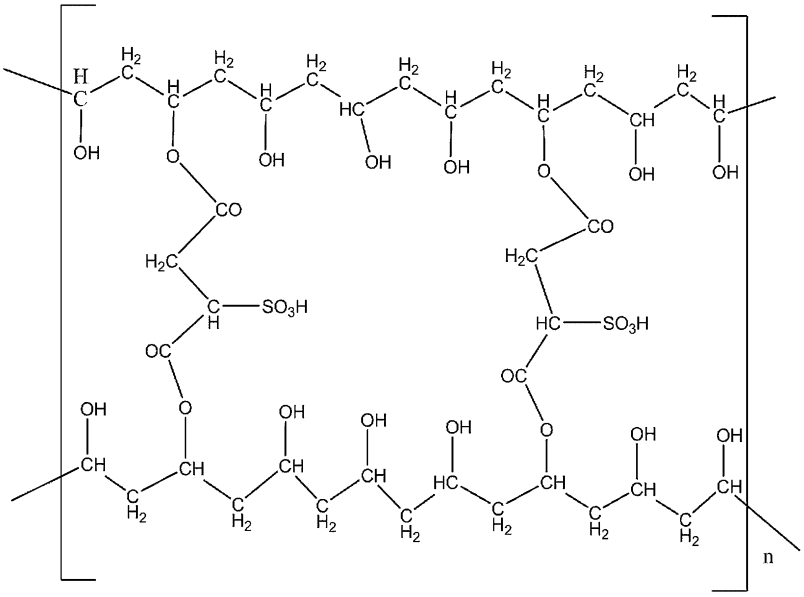

Possible crosslinking structure of PVA/PSSA and SSA

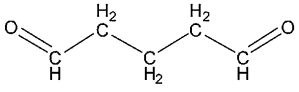

Glutaraldehyde (GA)

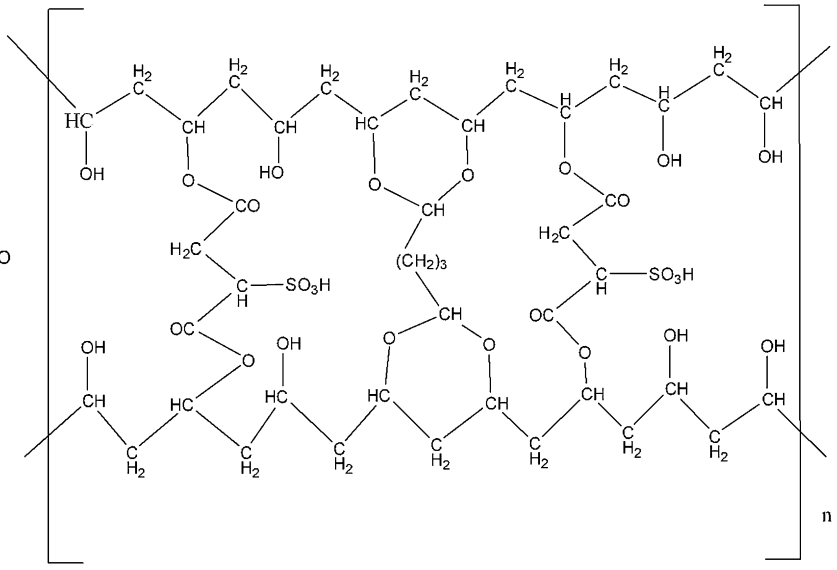

Scheme 3. Possible structure of the PVA–SSA–GA membrane by two-step crosslinking.

measuring methanol permeation, the membrane is immersed in pure water at least for two days, and then clamped between the well-stirred donor (chamber A) and receptor (chamber B) compartments with a membrane cross-sectional area of 0.25π cm^2 exposed to both compartment solutions. Chamber B (V = 100 mL) is filled with water, while chamber A (V = 100 mL) is filled with a molar methanol solution. Methanol concentration in chamber B is determined by a refractive index (RI) at different times [21]. Methanol permeability is then calculated from the curve of methanol concentration versus time.

3. Results and discussion

3.1. Structure of the PVA–SSA–GA membrane

Esterized crosslinking between PVA and SSA forms the primitive membrane. Most crosslinking constitutes the inner network structure. The SO_3H groups of the SSA and OH groups of the PVA are hydrophilic. When SSA content is high (and the molar ratio of SO_3H/OH exceeds 0.1), the network membrane dissolves in water. The second step involves crosslinking between PVA and GA. This second step generates an acetal ring group and/or ether linkage over most of the outer surface membrane, forming a hydrophobic protective layer. The aforementioned membrane becomes water-insoluble even when the molar ratio of SO_3H/OH exceeds 0.45. No significant mass loss while immersing the membrane in DI water for approximately 300 days proves this result: the water remains clean and the membrane completely insoluble. This two-step crosslinking yields a membrane highly stable in water and also improves proton conductivity and prevents methanol crossover, as discussed later. Scheme 3 presents the possible structure of the PVA–SSA–GA membrane by this two-step crosslinking.

3.2. IR spectra of PVA–SSA–GA membranes

Table 1 presents ATR IR spectral vibration modes of the PVA–SSA membrane containing 0.152 (1-PVA–SSA), 0.222 (2-PVA–SSA), 0.293 (3-PVA–SSA), 0.364 (4-PVA–SSA) molar ratio of SSA/OH. Fingerprints of the PVA–SSA membrane at 550–673 cm^{-1} attribute to the wagging and rocking vibration of $(-CH_2)_2$. The peak at 707 cm^{-1} corresponds to $-CH_2$ vibration, and the weak IR peak at 803 cm^{-1} is assigned to the C–S stretching vibration [3]. The peaks at 970, 983 and 1092 cm^{-1} correspond to C–O–C stretching vibrations [3]. The peaks at 1031–1056 cm^{-1} attribute to symmetry vibration of the sulfonic group [3]. Unfortunately, the asymmetric vibrations, doubly degenerated or not according to $-SO_3^-$ group asymmetry and expected in the IR frequency range at approximately 1163 cm^{-1}, are obscured by the intense C–O–C stretching vibration and cannot be located precisely. Peaks at 1211–1224 cm^{-1} associate with the symmetric stretching vibration of the $-SO_3^-$ group and the stretching vibration of C–O–C. The broadening of the peak at 1404 cm^{-1} of the pristine PVA–SSA membrane represents the $-SO_3^-$ group stretching vibration [22]. Peak appearance of the pristine sample at around 1632 cm^{-1} attributes to the bending vibration of the –OH group bonded with the $-SO_3^-$ group, indicating that some water is present in the hydrophilic domains of the pristine PVA–SSA–GA membrane [22]. The peak at 1713 cm^{-1} of the pristine PVA–SSA membrane represents the –C=O group stretching vibration. Peak broadening at 3242–3374 cm^{-1} of the pristine PVA–SSA membrane represents the –OH group stretching vibration.

Table 1
Assignments of the ATR IR (500–4000 cm^{-1}) peaks of PVA–SSA–GA membranes.

Assignments	Wave no.
$\omega(-CH_2)_2$	550–673 s
$\upsilon(-CH_2)$	707 sh, m
υ(C–S)	803 vw
υ(C–S)	851 vw
υ_s(C–O–C)	970 vw
υ(C–O–C)	983 m
υ(C–O–C)	1092 w
$\upsilon_s(SO_3^-)$	1031–1056 vs
υ(C–O–C), $\upsilon_{as}(SO_3^-)$	1163 vs
υ(C–O–C), $\upsilon_s(SO_3H)$	1211 vs
$\upsilon_s(SO_3H)$	1224 vs
υ(C–C)	1302 m
υ(C–C)	1318 m
δ(CH)	1378 m
$\upsilon_{as}(SO_3H)$	1404 m
δ(OH)	1632 s
υ(C=O)	1713 s
$\upsilon_s(CH_2)$	2908 s
$\upsilon_s(CH_2)$	2942 s
υ(OH)	3242 vs, b
υ(OH)	3374 vs, b

s: strong; m: medium; w: weak; sh: shoulder; v: very; b: broad.
δ: scissoring vibration; ω: wagging and rocking vibration.
υ: vibration; υ_s: symmetry vibrations; υ_{as}: asymmetry vibrations.

Fig. 1(a)–(c) presents the ATR IR spectrum of the PVA–SSA–GA membrane. These membranes with SO_3H/OH = 0.152, 0.222, 0.293, 0.364 molar ratio, exhibit no spectral characteristic of the aldehyde –CH group at 2720 cm^{-1} when the second chemical crosslinking of PVA–SSA reacts with glutaraldehyde (GA) after heat treatment, revealing that the second crosslinking forms a successful membrane reaction. Peak intensity at approximately 2920–2980 cm^{-1} increases with second crosslinking duration because of the $-CH_2$ vibration of the acetal ring and/or ether linkage. The peak at about 2852–2858 cm^{-1} corresponds to the –CH vibration of the acetal ring and/or ether linkage. Fig. 1(a) and (b) presents that peak intensity of the pristine PVA–SSA membrane at 1130–1160 cm^{-1} and 1224–1236 cm^{-1} increase, corresponding to the SO_3H groups and C–O–C stretching vibrations of the ester linkage between SSA and PVA. Fig. 1(c) shows that the peaks of the sample 2-PVA–SSA–GA–C1 at 1080–1130 cm^{-1} and 1142–1152 cm^{-1}, corresponding to the C–O–C stretching vibrations of the acetal ring and the formation of an ether linkage with second crosslinking between GA and PVA, increase in intensity. On the other hand, the peaks of the samples 3-PVA–SSA–GA–C1 and 4-PVA–SSA–GA–C1 at 1080–1130 cm^{-1} and 1142–1152 cm^{-1} are relatively weak in intensity compared to 2-PVA–SSA–GA–C1. This is ascribed to the fact that there are more linkages formed through the first crosslinking step with SSA than those through the second step with GA for both 3-PVA–SSA–GA–C1 and 4-PVA–SSA–GA–C1 samples. The first crosslinking also increases proton conductivity, methanol permeability, water uptake and ion exchange. The increased single/bridge esterization ratio between PVA and SSA molecules and the amount of SSA lead to increased methanol permeability [6].

3.3. Thermal analysis

Fig. 2(a) and (b) presents the DSC curves of PVA–SSA–GA membranes at various molar ratios of SO_3H/OH. All membranes are crosslinked with GA for 1 or 2 h, and then heat-treated for 2 h. Generally speaking, the membranes exhibit an increased endothermic heat flow at 50–100 °C with increase of SO_3H/OH value, indicating the membranes with more SO_3H groups will associate with more free water. The endothermic heat flow at 100–150 °C demonstrates vaporization of bound water. The peaks shifting towards lower temperature at higher SO_3H/OH value indicates that loosely bound water increase as the number of hydrophilic SO_3H group increases. As shown in Fig. 2(b), the 2-PVA–SSA–GA–C2H2 sample, being a dense membrane, associates with less free water. The possible reason is that it possesses a suitable distribution of ester linkages inside and acetal rings or ether linkages outside. A hydrophobic protective surface layer associated with less free water. The 1-PVA–SSA–GA–C1H2 and 2-PVA–SSA–GA–C2H2 samples associate with least water. This can be further demonstrated as follows.

Fig. 3 (a) and (b) plots the TGA curves of PVA–SSA–GA membranes at various SO_3H/OH molar ratios. All membranes are crosslinked with GA for 1 or 2 h and then heat-treated for 2 h. The membranes exhibit increased weight loss at 40–110 °C and an increased SO_3H/OH molar ratio, indicating that more SO_3H groups associate with more free water. The weight loss at 120–170 °C reveals vaporization of bound H_2O. A shift towards

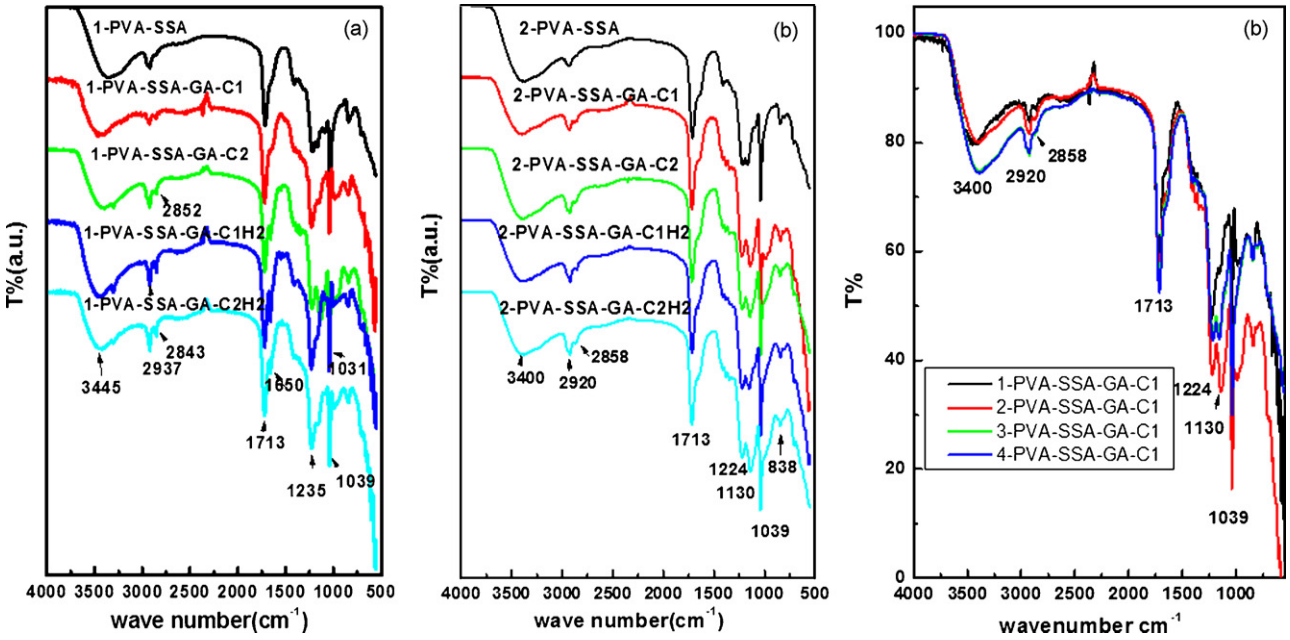

Fig. 1. ATR IR spectra of the membrane with various molar ratios of SSA/OH: (a) 0.152, (b) 0.222; 1-PVA–SSA and 2-PVA–SSA: without the second crosslinking step and heat treatment; C1 and C2: with the second crosslinking step for 1 and 2 h, respectively but without heat treatment; H2: with the second crosslinking step followed by heat treatment for 2 h. (c) ATR IR spectra of the membranes with various molar ratios of SSA/OH = 0.152 (1-PVA–SSA–GA–C1), 0.222 (2-PVA–SSA–GA–C1), 0.293 (3-PVA–SSA–GA–C1), 0.364 (4-PVA–SSA–GA–C1) for the second crosslinking step.

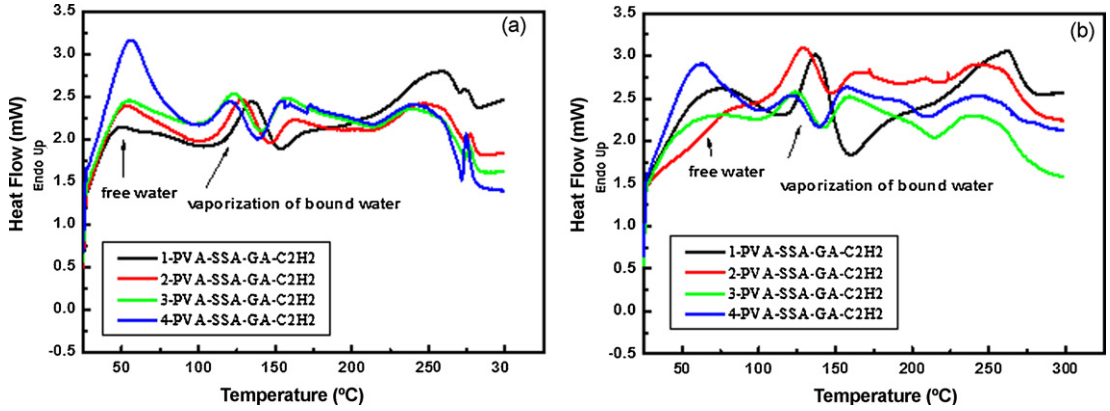

Fig. 2. DSC curves of PVA–SSA–GA membranes at different molar ratios of SO_3H/OH: (a) membranes crosslinked with GA for 1 h and followed by heat treatment for 2 h; (b) membranes crosslinked with GA for 2 h and followed by heat treatment for 2 h.

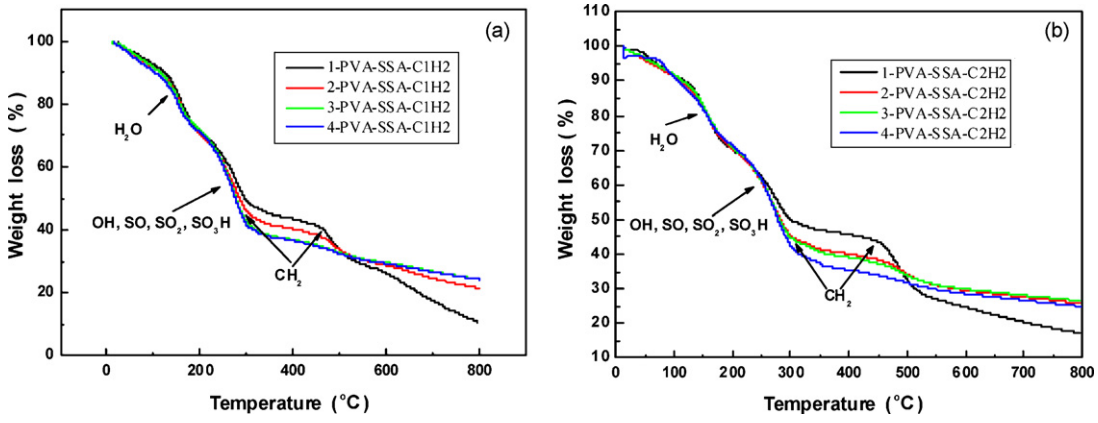

Fig. 3. TGA curves of PVA–SSA–GA membranes at different molar ratios of SO_3H/OH.

Table 2
Water uptake of membranes with various SO_3H/OH molar ratios.

Sample	SO_3H/OH (molar ratio)	Water uptake ($g\,g^{-1}$)	Free water (%)	Bound water (%)
1-PVA–SSA–GA–C1H2	0.152	0.33	0.64	99.36
2-PVA–SSA–GA–C1H2	0.222	0.723	17.02	82.98
3-PVA–SSA–GA–C1H2	0.293	1.27	13.14	86.86
4-PVA–SSA–GA–C1H2	0.364	1.56	14.25	85.75
1-PVA–SSA–GA–C2H2	0.152	0.34	3.02	96.99
2-PVA–SSA–GA–C2H2	0.222	0.79	4.21	95.79
3-PVA–SSA–GA–C2H2	0.293	1.15	5.57	94.43
4-PVA–SSA–GA–C2H2	0.364	1.42	15.03	84.97

low temperature with a high SO_3H/OH molar ratio, as the number of SO_3H groups increase, suggests the vaporization of loosely bound water. Weight loss at 220–304 °C demonstrates the decomposition of OH, SO_2, SO, SO_3H and CH_2 and weight loss increases with the SO_3H/OH molar ratio. Weight loss at 460–523 °C is caused by CH_2 decomposition, evidenced only in samples 1-PVA–SSA–GA–C1H2, 1-PVA–SSA–GA–C2H2, 2-PVA–SSA–GA–C1H2 and 2-PVA–SSA–GA–C2H2. A decomposition shift to low temperature is caused by an increased SO_3H/OH molar ratio, as increasing numbers of SO_3H groups indicate likely decomposition of OH, SO_2, SO and SO_3H groups.

3.4. Water state and ion exchange capacity

Table 2 shows that water uptake of membranes increases with the SO_3H/OH molar ratio. Table 3 shows that ion exchange capacity of the membranes increases with the SO_3H/OH molar ratio. Ion exchange capacity of 2.676 m mol g^{-1} is the highest among synthesized membranes, exceeding that of Nafion®. Water uptake and ion exchange capacity of PVA–SSA–GA membranes are good, associated with good proton conductivity. Table 2 presents high water uptake and high bound water/free water ratio. The amount of water uptake and the ratio exceed those of any previously described PVA–based electrolyte [5–17]. Ion exchange capacity of membranes, also given in Table 3, demonstrates that most samples have higher ion exchange capacity than other previously described PVA–based electrolytes [5,7,10,11,14–16].

Detecting the water state of membranes involves melting transitions in DSC measurements. Fig. 4(a) and (b) plots the results. Endothermic heat flow increases with the SO_3H/OH molar ratio. The heat flow indicates the amount of freezing water [11,19,20]. Fig. 4(a) and (b) presents the amazing release of heat flow at low temperature, revealing ice crystal formation at −10 to −20 °C as the number of SO_3H groups increases. Water molecules in the ice crystal formed at −10 to −20 °C bond with the SO_3H groups. The amount of freezing water and ice crystals decreases with the increasing duration of the second crosslinking step between PVA and GA. This result confirms that the dense membrane structure and the hydrophobic protective layer form in the second step of crosslinking with GA.

3.5. Proton conductivity and methanol permeability

Table 3, Fig. 5(a) and (b) present the methanol permeability and proton conductivity of membranes with various SO_3H/OH molar ratios. The membranes are crosslinked with 0.5 M GA in an acetone solution for 1 or 2 h followed by heat treatment for 2 h at 35 °C. The highest proton conductivity observed among the synthesized membranes at room temperature is 5.26×10^{-2} S cm^{-1}, exceeding that of the Nafion® membrane. Methanol permeability of the synthesized membranes is approximately 1×10^{-7} cm^2 S^{-1}. The current study obtained better selectivity for the membranes with the second crosslinking step continued for 2 h, than with that

Table 3
Methanol permeability, proton conductivity and ion exchange capacity of membranes with various SO_3H/OH molar ratios.

Sample	SO_3H/OH (molar ratio)	Ion exchange capacity (m mol g^{-1})	Methanol permeability, p (10^{-7} cm^2 S^{-1})	Proton conductivity, σ (S cm^{-1})	Selectivity, σ/p (10^5 S^2 cm^{-3})
1-PVA–SSA–GA–C1H2	0.152	0.576	1.4	0.0101	7.2143
2-PVA–SSA–GA–C1H2	0222	1.231	2.17	0.0212	9.7696
3-PVA–SSA–GA–C1H2	0.293	2.345	3.44	0.0356	10.3488
4-PVA–SSA–GA–C1H2	0.364	2.676	6.37	0.0388	6.0911
1-PVA–SSA–GA–C2H2	0.152	0.677	0.55	0.0100	18.1818
2-PVA–SSA–GA–C2H2	0.222	1.261	1.17	0.0277	23.6375
3-PVA–SSA–GA–C2H2	0.293	2.387	2.46	0.0389	15.813
4-PVA–SSA–GA–C2H2	0.364	2.433	3.53	0.0526	14.9008
PVA			29.0	0.0001	0.00034
Nafion® 117		0.91[a]	14.9	0.0134	0.09

[a] Data obtained from Ref. [23].

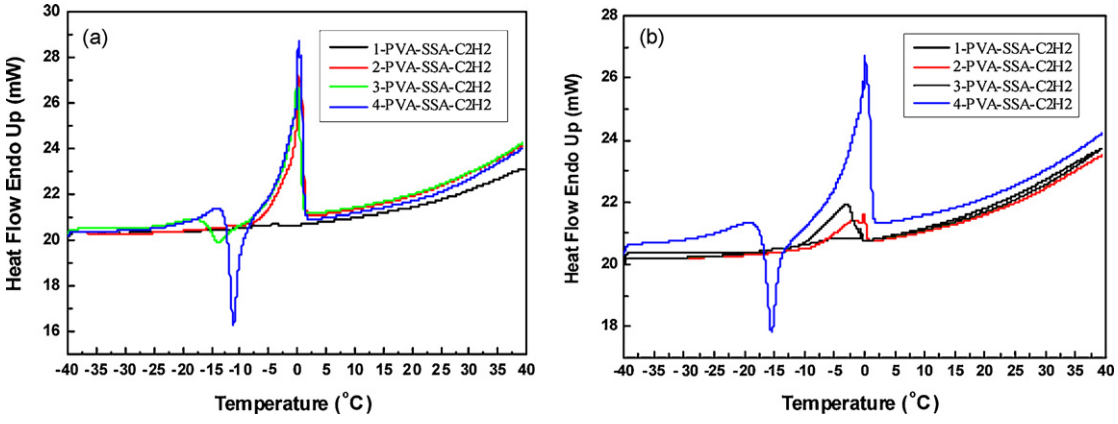

Fig. 4. DSC curves of PVA–SSA–GA membranes.

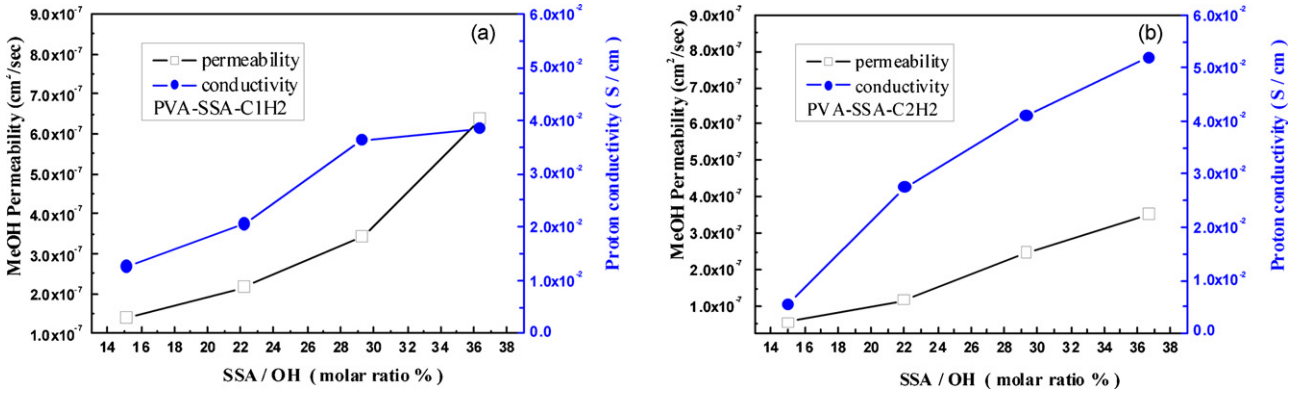

Fig. 5. Methanol permeability and proton conductivity of PVA–SSA–GA membranes at different molar ratio percentages of SO_3H/OH.

obtained with crosslinking for 1 h; the 2-PVA–SSA–GA–C2H2 membrane demonstrates the best selectivity. The second crosslinking step effectively prevents methanol permeability. This study indicates higher SSA content (and the molar ratio of SO_3H/OH exceeds 0.1) if the second crosslinking step with GA is eliminated, dissolving the membrane in water and methanol. A similar phenomenon occurs when performing the second crosslinking step with GA without a first crosslinking step. The membranes then dissolve in both water and methanol.

4. Conclusion

Poly(vinyl alcohol) (PVA)–sulfosuccinic acid(SSA)–glutaraldahyde(GA) electrolyte membranes, synthesized by the two-step crosslinking process, involving esterization and formation of an acetal ring group or ether linkage, show better properties than the electrolytes synthesized by a one-step crosslinking process and even Nafion. This work uses SSA as the first crosslinking and sulfonating agent to simultaneously promote formation of an inter-crosslinked structure and sulfosuccinic acid functional groups that support proton conductivity. Using GA as the second crosslinking agent, reacted with the spare OH group of PVA, promotes formation of a dense membrane structure and hydrophobic protective layer, indicating a heightened methanol barrier. The structure of PVA–SSA–GA membranes is stable in water and strongly bonds therein.

Acknowledgement

The authors gratefully acknowledge the financial support of the National Science Council (under contract numbers NSC96-2221-E-011-061, and NSC96-2120-M-011-001), facilities from the National Synchrotron Radiation Research Center (NSRRC), and the National Taiwan University of Science and Technology, Taiwan, ROC.

References

[1] J.J. Sumner, S.E. Creager, J.J. Ma, D.D. DesMarteau, J. Electrochem. Sci. 145 (1998) 107–110.
[2] S. Slade, S.A. Campbell, T.R. Ralph, F.C.J. Walsh, J. Electrochem. Sci. 149 (2002) 1556–1564.
[3] A. Gruger, A. Regis, T. Schmatko, P. Colomban, Vib. Spectrosc. 26 (2001) 215–225.
[4] Y.F. Lin, C.Y. Yen, C.C.M. Ma, S.H. Liao, C.H. Lee, Y.H. Hsiao, H.P. Lin, J. Power Sources 171 (2007) 388–395.
[5] Akita, Hiroshi, K.K., Honda Gijyutsu Kenkyusho, Wako-shi, Saltama 351-0193(JP) E.P. Patent 1085051 (2001).
[6] J.W. Rhim, H.B. Park, C.S. Lee, J.H. Jun, D.S. Kim, Y.M. Lee, J. Membr. Sci. 238 (2004) 143–151.
[7] R.K. Nagarale, G.S. Gohil, V.K. Shahi, R. Rangarajan, Macromolecules 37 (2004) 10023–10030.
[8] T. Uragami, K. Okazaki, H. Matsugi, T. Miyata, Macromolecules 35 (2002) 9156–9163.
[9] D.S. Kim, H.B. Park, J.W. Rhim, Y.M. Lee, J. Membr. Sci. 240 (2004) 37–48.
[10] D.S. Kim, H.B. Park, J.W. Rhim, Y.M. Lee, Solid State Ionics 176 (2005) 117–126.
[11] T. Qiao, T. Hamaya, T. Okada, Chem. Mater. 17 (2005) 2413–2421.
[12] W. Charles, J. Wlker, J. Electrochem. Sci. 151 (2004) 1797–1803.
[13] M.S. Kang, J.H. Kim, J. Won, S.H. Moon, Y.S. Kang, J. Membr. Sci. 247 (2005) 127–135.
[14] D.S. Kim, M.D. Guiver, S.Y. Nam, T.I. Yun, M.Y. Seo, S.J. Kim, H.S. Hwang, J.W. Rhim, J. Membr. Sci. 281 (2006) 156–162.
[15] C.W. Lin, Y.F. Huang, A.M. Kannan, J. Power Sources 164 (2007) 449–456.
[16] C.W. Lin, Y.F. Huang, A.M. Kannan, J. Power Sources 171 (2007) 340–347.
[17] C.K. Yeom, K.H. Lee, J. Membr. Sci. 109 (1996) 257–265.
[18] C. Manea, M. Mulder, J. Membr. Sci. 206 (2002) 443–453.
[19] L.E. Karlsson, B. Wesslen, P. Jannasch, Electrochim. Acta 47 (2002) 3269–3275.
[20] D.I. Ostrovskii, L.M. Torell, M. Paronen, S. Hietala, F. Sundholm, Solid State Ionics 97 (1997) 315–321.
[21] S.P. Tung, B.J. Hwang, J. Membr. Sci. 241 (2004) 315–323.
[22] R. Buzzoni, S. Bordiga, G. Ricchiardi, G. Spoto, A. Zecchina, J. Phys. Chem. 99 (1995) 11937–11951.
[23] K.D. Kreuer, J. Membr. Sci. 185 (2001) 29–39.